

Combustion-Derived Ultrafine Particles Transport Organic Toxicants to Target Respiratory Cells

Arthur Penn,¹ Gleeson Murphy,¹ Steven Barker,¹ William Henk,¹ and Lynn Penn²

¹Department of Comparative Biomedical Sciences, Louisiana State University, School of Veterinary Medicine, Baton Rouge, Louisiana, USA; ²Department of Chemical and Materials Engineering, University of Kentucky, Lexington, Kentucky, USA

Epidemiologic evidence supports associations between inhalation of fine and ultrafine ambient particulate matter [aerodynamic diameter $\leq 2.5 \mu\text{m}$ ($\text{PM}_{2.5}$)] and increases in cardiovascular/respiratory morbidity and mortality. Less attention has been paid to how the physical and chemical characteristics of these particles may influence their interactions with target cells. Butadiene soot (BDS), produced during combustion of the high-volume petrochemical 1,3-butadiene, is rich in polynuclear aromatic hydrocarbons (PAHs), including known carcinogens. We conducted experiments to characterize BDS with respect to particle size distribution, assembly, PAH composition, elemental content, and interaction with respiratory epithelial cells. Freshly generated, intact BDS is primarily (> 90%) PAH-rich, metals-poor (nickel, chromium, and vanadium concentrations all < 1 ppm $\text{PM}_{2.5}$, composed of uniformly sized, solid spheres (30–50 nm) in aggregated form. Cells of a human bronchial epithelial cell line (BEAS-2B) exhibit sequential fluorescent responses—a relatively rapid (~ 30 min), bright but diffuse fluorescence followed by the slower (2–4 hr) appearance of punctate cytoplasmic fluorescence—after BDS is added to medium overlying the cells. The fluorescence is associated with PAH localization in the cells. The ultrafine BDS particles move down through the medium to the cell membrane. Fluorescent PAHs are transferred from the particle surface to the cell membrane, cross the membrane into the cytosol, and appear to accumulate in lipid vesicles. There is no evidence that BDS particles pass into the cells. The results demonstrate that uptake of airborne ultrafine particles by target cells is not necessary for transfer of toxicants from the particles to the cells. **Key words:** cytoplasmic vesicles, PAHs, polynuclear aromatic hydrocarbons, punctate fluorescence, respiratory epithelium, soot, ultrafine particles. *Environ Health Perspect* 113:956–963 (2005). doi:10.1289/ehp.7661 available via <http://dx.doi.org/> [Online 6 May 2005]

Increased morbidity and mortality have been associated with exposure to inhaled airborne particulate matter (PM; Dockery et al. 1993; Samet et al. 2000; Schwartz et al. 1996). In 1997, the U.S. Environmental Protection Agency (EPA) issued revised National Ambient Air Quality Standards (U.S. EPA 1997) for airborne PM, which supplemented the 1991 standards (U.S. EPA 1991) by focusing on PM with aerodynamic diameters $\leq 2.5 \mu\text{m}$ ($\text{PM}_{2.5}$). Small increases in levels of ambient $\text{PM}_{2.5}$ result in increases (> 1%) in cardiovascular and respiratory mortality (Pope et al. 2002). Recently, the focus has begun to shift to health effects arising from inhalation of ultrafine particles (diameter < 0.1 μm) that comprise a small fraction of the total mass, but most of the total number, of airborne PM (Peters et al. 1997). For equivalent masses of inhaled particles, ultrafine particles provide a greater surface area for adsorption of potentially toxic agents than do the larger sized particles.

Inhaled ultrafine particles can be deposited in the lung and can migrate from there into systemic circulation and thus to the heart, as well as to more distal organs. Within 5 min of intratracheal instillation, 25–30% of ^{99m}technetium-labeled albumin ultrafine particles (nominal diameter $\leq 80 \text{ nm}$) were detected in the blood (Nemmar et al. 2001).

Ambient fine and ultrafine particles arise from multiple sources, both combustion-related (e.g., diesel, petrochemical), and non-combustion-related (e.g., crustal, agricultural). The fine soot particles arising from incomplete combustion of coal and petroleum have been associated with increased mortality (Laden et al. 2000). In urban settings, diesel exhaust is a prominent source of fine particles (U.S. EPA 2002). Organic solvent extracts of diesel exhaust particles (DEPs) induce oxidative stress in respiratory epithelial cells and macrophages (Li et al. 2002). Particle-rich diesel exhaust contains relatively high levels of polynuclear aromatic hydrocarbons (PAHs), including the well-characterized carcinogen benzo(a)pyrene (BaP). Other contributors to the burden of airborne particulates include PM arising from flaring of volatile hydrocarbons at refineries and/or incomplete combustion of unused or fugitive hydrocarbons at petrochemical plants. These additional sources of inhalable, PAH-rich particles are of special concern where refineries and/or petrochemical processing plants are concentrated.

1,3-Butadiene (BD) is a volatile, “top 40” U.S. production chemical [$> 3 \times 10^9 \text{ lb}$ produced annually; Occupational Safety and Health Administration (OSHA) 2004]. Industrial petrochemicals, including BD, that escape the production stream or that remain

unreacted are burned. The butadiene soot (BDS) produced during incomplete combustion of BD is a complex, PAH-rich mixture of particulates. A broad size range of PAHs [up to ~ 1,000 atomic mass units (amu)], including BaP and other carcinogens, is present in BDS. After incubation with BDS extracts in dimethylsulfoxide (DMSO), normal human bronchial epithelial cells, which are putative target cells for inhaled irritants, exhibited plasma membrane blebbing, small but statistically significant increases in the number of binucleate cells, and a diffuse cytoplasmic fluorescence when viewed under the light microscope (Catallo et al. 2001).

There is a growing literature on the pathologic responses of cells of the respiratory and cardiovascular systems after exposure to ultrafine particles (Bermudez et al. 2004; Chalupa et al. 2004; Dick et al. 2003; Nemmar et al. 2004). Less attention however, has been paid to how the detailed physical and chemical characteristics of combustion-derived ultrafine particles influence interactions of these particles and their constituents with target cells. Here, we characterize BDS with respect to particle size distribution and assembly, PAH composition, and elemental content of BDS ultrafine particles. We also describe *in vitro* assays that demonstrate that BDS ultrafine particles can transport and transfer adsorbed organic constituents directly to target respiratory cells, without uptake of the particles by the cells.

Materials and Methods

Generation of BDS. We brought a tank of BD (Aldrich, St. Louis, MO) that had been stored at -20°C to room temperature. The BD ($\geq 99\%$ purity) contained approximately 175 ppm *t*-butylcatechol as an inhibitor. The BD gas was passed through a back-flash-protected stainless steel two-stage regulator to

Address correspondence to A. Penn, Department of Comparative Biomedical Sciences, Louisiana State University, School of Veterinary Medicine, Skip Bertman Dr., Baton Rouge, LA 70803 USA. Telephone: (225) 578-9760. Fax: (225) 578-9895. E-mail: apenn@vetmed.lsu.edu

We thank T. Ahlert, M. Faubion, O. Borkhsenius, and C. David for their technical assistance.

This work was supported by a grant from the Louisiana Governor's Biotechnology Initiative.

The authors declare they have no competing financial interests.

Received 13 October 2004; accepted 14 April 2005.

a stainless steel Bunsen burner (aperture, 0.85 mm inner diameter; feed pipe, 10 cm). The flame was adjusted until a plume of black smoke rose from the top of the burner. Combustion was carried out in a fume hood with active ventilation. The BD feed rates were 5–7 mL/sec under normal atmosphere, with flame heights of approximately 1 cm. We captured the particles passing through the feed pipe on cellulose filters held within a Buchner funnel positioned approximately 15 cm above the pipe outlet and attached to a vacuum pump. The BDS was scraped gently off the filters and stored in aluminum-foil-wrapped glass vials capped with foil-lined lids.

We qualitatively determined the success of each BDS-generating reaction by assessing PAH-associated fluorescence of the product. We extracted 1 mg BDS with 2 mL dichloromethane (DCM; Optima; Fisher, Fairlawn, NJ) for 1 min. Fluorescence of the extract was detected under ultraviolet (UV) light (320 nm excitation).

Particle size analysis. The sampling train was set up for size fractionation of BDS particles as follows: burner, RespiCon virtual sampler (TSI; St. Paul, MN), in-line HEPA filter, digital flow meter, Magnahelic (Dwyer, Michigan City, IN), and house vacuum. Size fractionation was carried out with a RespiCon virtual sampler that was set approximately 15 cm above the top of the burner. The first stage of the RespiCon collected particles < 2.5 μm ; the second and third stages collected particles 2.5–10 μm and > 10 μm , respectively. Preweighed filters from each impactor stage were weighed, photographed, and submitted for extraction and gas chromatography/mass spectrometry (GC/MS) analyses for PAHs.

Elemental analyses. All elemental analyses were carried out by Quantitative Technologies Inc. (Whitehouse, NJ). Carbon, hydrogen, and nitrogen content were determined with a Perkin-Elmer CHN elemental analyzer (model 2400; PerkinElmer, Wellesley, MA). Samples in the analyzer were combusted in a pure oxygen environment. Product gases were separated under steady-state conditions and measured as a function of thermal conductivity. Sulfur was converted to sulfate and then titrated versus standards, with an indicator. Oxygen in BDS was determined with the elemental analyzer fitted with an oxygen accessory kit. The oxygen in the organic starting material was converted by pyrolysis to carbon monoxide, which was separated from other pyrolysates under steady-state conditions and measured as a function of thermal conductivity.

Freshly prepared BDS samples were analyzed by inductively coupled plasma (ICP) spectrometry for the presence of 64 additional elements. Samples were digested with nitric

acid in a CEM 2100 microwave oven (CEM, Matthews, NC) and then diluted to volume with 18 Mohm-cm water. Reagent blanks were prepared similarly. Samples were analyzed with a Perkin-Elmer Optima 3000XL ICP spectrometer (PerkinElmer) that had been calibrated with traceable standards from the National Institute of Standards and Technology (NIST) (Gaithersburg, MD). The resulting calibration was confirmed by analysis of an independently prepared calibration check standard. A method blank was analyzed, and its value was subtracted from all sample analyses. Iron concentrations were determined in pristine reaction vessels in which the level of iron, if any, was below the limit of detection. Of the 64 elements screened, 52, including chromium, nickel, and vanadium, were present at levels < 1 ppm.

Percentage of adsorbed organic components. Three 50-mg samples of BDS, in mini-Buchner funnels fitted with preweighed Whatman #1 filters, were each extracted via vacuum filtration with five successive 10-mL aliquots of DCM. The filters were reweighed after drying in air.

GC/MS analysis of PAH components of BDS particles. The BDS generated by controlled combustion of BD was collected on glass-fiber filters and analyzed for PAHs by GC/MS. An unused filter (negative control) and a solvent-only method blank also were analyzed. The BDS (1 mg) was placed into a 10-mL Pyrex conical tube fitted with a Teflon-lined screw cap. The DCM (2.0 mL, ultra-high-purity grade; Aldrich), was added to each tube after being "spiked" with deuterated NIST reference standards for several PAHs previously identified in BDS (Catalo et al. 2001): naphthalene-d₈ (5 $\mu\text{g}/\text{mL}$), anthracene-d₁₀ (1 $\mu\text{g}/\text{mL}$), chrysene-d₁₂ (1 $\mu\text{g}/\text{mL}$), BaP-d₁₂ (5 $\mu\text{g}/\text{mL}$), and perylene-d₁₂ (2 $\mu\text{g}/\text{mL}$). The tubes were capped and heated (40°C for 4 hr) in a sand bath. A 200- μL aliquot of each sample extract was filtered through a 0.45- μm nylon filter (Nalgene, Rochester, NY) that had been fitted onto a 1-mL syringe barrel. The filtered samples were placed in conical glass sample vial inserts and submitted for GC/MS analysis. Three sets of BDS PM_{2.5} were analyzed by GC/MS after extraction with DCM. There was insufficient material for analysis in the PM₁₀ and larger fractions.

The GC/MS analyses were conducted with an Agilent 5973 mass selective detector/6890 GC/data system (Agilent, Palo Alto, CA) in full scan (40–600 amu), positive ion, electron impact mode. Splitless injections of 1 mL were made onto a 28 m \times 0.25 mm, 0.25- μm film thickness, DB5 fused silica glass capillary column (Agilent), with the purge function initiated at 0.75 min postinjection. The injector temperature was 250°C. The initial column temperature (50°C) was held for

5 min, ramped at 10°C/min to 300°C, and held there for 10 min. The transfer zone of the instrument was held at 320°C, and the source temperature was 200°C. Full-scan spectra were compared with reference library spectra and retention indices (relative to deuterated internal standards) to determine peak identity. The most abundant PAH peak areas were integrated and compared by ratio with the corresponding peak area for the anthracene-d₁₀ internal standard. Four compounds (anthracene, chrysene, benzopyrenes, and perylene) were identified directly by comparison with each of their respective deuterated standards.

Scanning electron microscopy of freshly prepared BDS. The BDS was collected from a plume by passing ethanol-cleaned, 12-mm, circular glass coverslips through the plume. The coverslips were affixed to aluminum stubs with conductive adhesive, sputter-coated with approximately 20 nm gold/palladium and examined by scanning electron microscopy (SEM; FEI Quanta 200 ESEM; FEI, Hillsboro, OR) at 20 kV. Digital images of 1,024 \times 884 pixels were recorded.

Transmission electron microscopy of freshly prepared BDS. Samples of BDS were collected directly from the plume onto 300-mesh, parlodion-coated copper grids that were examined by transmission electron microscopy (TEM; Zeiss EM-10C; Zeiss, Thornwood, NY). To simulate the processing of BEAS-2B cells, freshly prepared BDS was collected on filters, transferred to clean tubes, passed through an ethanol series (50–100%), and infiltrated with epoxy resin. The polymerized resin was sectioned and then examined as described above.

Cell culture. BEAS-2B cells are a non-tumorigenic line derived from normal human bronchial epithelial cells (Ke et al. 1988). BEAS-2B cells (1–1.5 \times 10⁶) were seeded into T-25 flasks (Corning, Corning, NY) containing bronchial-epithelial growth medium (BEGM), before expansion in T-150 flasks. BEGM is a basal medium (BioWhittaker, Rockland, ME) supplemented (per 500 mL) with 2 mL of 13 mg/mL bovine pituitary extract and 0.5 mL each 0.5 mg/mL hydrocortisone, 0.5 $\mu\text{g}/\text{mL}$ human recombinant epidermal growth factor, 0.5 mg/mL epinephrine, 10 mg/mL transferrin, 5 mg/mL insulin, 0.1 $\mu\text{g}/\text{mL}$ retinoic acid, 6.5 $\mu\text{g}/\text{mL}$ triiodothyronine, 50 mg/mL gentamicin, and 50 $\mu\text{g}/\text{mL}$ amphoterin-B. Cells were grown to 80–90% confluence (37°C, 5% CO₂/95% air), split into 60-mm dishes (\sim 2.5 \times 10⁵ cells/dish), and expanded until approximately 70% confluent. Medium was changed immediately before BDS addition.

BDS exposures. Unextracted soot particles. For approximation of routine *in vivo* exposure conditions to airborne particles, the BDS was

not subjected to charge neutralization before addition to cell cultures. The BDS (3 mg) was sprinkled onto the surface of the BEGM overlying the BEAS-2B cells. Cells were incubated from 5 min to 72 hr. Unless otherwise noted, the BDS was not removed nor was the medium changed during the course of the exposures. Unexposed cells served as negative controls. Cells sprinkled with 0.5 mg crystalline BaP served as solid PAH controls. Cells to which 40 μ L of a 5-mM BaP solution (in DMSO) was added to 5 mL BEGM, served as fully solubilized PAH controls. Cells with 3 mg graphite (> 98% pure; Sigma, St. Louis, MO) sprinkled directly onto the surface of the BEGM served as controls for cell responses to carbon particles lacking adsorbed organic compounds. In all cases, cell responses were determined with a fluorescence microscope (Zeiss Axiovert 405 M) equipped with a 100 W mercury lamp and a Zeiss 02 filter combination (365/420 nm) for excitation and emission.

Sonicated soot. For determination of whether disrupting the aggregated BDS ultrafine particles enhanced the responses of BEAS-2B cells, BDS was sonicated (Branson model 450 Sonifier; Branson Ultrasonics, Danbury, CT) in BEGM (3 mg/5 mL) before application to the cells. The output of the sonifier was at setting 5, with a constant-duty cycle and five consecutive 15-sec pulses, with swirling of the vessel between pulses. Diluted (1:10, 1:20, 1:50, 1:100) particle-BEGM suspensions were added to cells. The time course (15 min to 48 hr) of fluorescent responses of cells to sonicated BDS preparations was compared with that of cells exposed to non-sonicated BDS sprinkled on the surface of the medium.

Postextraction soot. For determination of whether organic extraction of soot altered the cell responses, the soot remaining on the Whatman filters (see "Percentage of adsorbed organic components," above) after extraction with DCM was collected and added to BEAS-2B cells (3 mg extracted soot/5 mL BEGM).

Soot extracts. For determination of whether soot extracts and intact BDS elicit similar cell responses over time, the DCM filtrate was dried under N_2 at room temperature and reconstituted in 1 mL DMSO. Aliquots (60 μ L) were mixed with 5 mL BEGM and added to BEAS-2B cells. Cells were examined for fluorescence responses (30 min to 48 hr).

Transwell incubations. The BEAS-2B cells were plated into wells of a 24-well plate ($\sim 2 \times 10^5$ cells/well). Transwell (Corning) inserts (0.4- μ m pores) were placed in each well. Medium (0.5–1.0 mL) and either BDS (0.3–0.6 mg) or soot extracts (50 μ L) were added to each Transwell, and cells were

viewed under a fluorescence microscope, as described above. Controls included *a*) wells with medium and cells but no BDS, *b*) wells with medium only, and *c*) wells with cells omitted and replaced with Octadecyl silane (ODS)-derivitized polymeric disks. At 48 hr, after aspiration of BEGM and rinsing of the wells with phosphate buffered saline (PBS), the Transwells and media were removed from the 24-well plates. ODS disks were washed with water, filter-extracted with DCM, and analyzed by GC/MS. Cells were rinsed with 0.2% trypsin in PBS and then removed from the wells by incubation with 0.2% trypsin in PBS at 37°C for 3 min. Cells were washed with PBS, pelleted, and extracted with DCM, as described above.

TEM of BEAS-2B cells exposed to BDS. The BEAS-2B cells, grown on Thermanox plastic coverslips (VWR International, West Chester, PA), were exposed for 42 hr to 0.6 mg BDS that had been sprinkled onto 1 mL BEGM in Transwells. Coverslips were washed with PBS and fixed with 1.25% glutaraldehyde/2% formaldehyde in 0.1 M sodium cacodylate. The coverslips were processed and examined as described above.

Table 1. Particle size distribution of BDS.

Particle size fraction	Percent in fraction (mean \pm SD) ^a
< 2.5 μ m	91.6 \pm 4.1
2.5–10 μ m	5.6 \pm 5.6
> 10 μ m	3.2 \pm 1.9

More than 90% of freshly generated BDS is of respirable size.
^aMean \pm SD of percent total mass found in each fraction; *n* = 5 replicates.

Table 2. Strong polyaromatic character of BDS revealed by elemental analysis.

Substrate	C	H	N	S	O
BDS	93.88 (0.37)	1.82 (0.07)	0.60 (0.31)	0.39 (0.02)	< 0.10
BDS (solvent washed)	95.95 (0.10)	0.78 (0.11)	0.11 (0.02)	0.35 (0.05)	0.55
Graphite	98.01	< 0.10	< 0.10	0.45	< 0.15

The results represent mean percentages \pm SEM for triplicate analyses.

Table 4. The 13 most prominent PAHs (152–276 amu) present in freshly generated BDS PM_{2.5}.

PAH	<i>m/z</i>	Ratio to IS (anthracene-d ₁₀)			Ratio to specific IS (mg/g soot)		
		1	2	3	1	2	3
Acenaphthylene	152	4.6	5.6	1.6			
Fluorene	166	1.4	2.5	0.8			
Anthracene	178	7.2	10.2	6.0	14.4	20.4	12.0
Cyclopentaphenanthrene	190	1.7	2.2	1.7			
Fluoranthene	202	6.2	6.4	6.7			
Acephenanthrylene	202	4.0	4.4	4.3			
Pyrene	202	8.0	9.6	8.7			
Benzofluorenes	216	1.0	2.0	1.0			
Acepyrene	226	7.6	7.2	9.8			
Chrysene	228	1.3	1.4	1.2	1.4	1.5	1.2
Benzopyrenes	252	2.0	2.2	2.5	1.7	2.0	1.7
Perylene	252	1.5	1.7	1.6	0.2	0.5	0.4
Benzoperylene/indeno[1,2,3-cd]pyrene	276	1.2	0.4	1.5			

IS, internal standards. The most abundant PAH peak areas were integrated and compared by ratio with the corresponding peak area for the anthracene-d₁₀ internal standard. Anthracene, chrysene, benzopyrenes, and perylene were identified directly by comparison with each of their respective deuterated standards.

Results

Generation of BDS. With BD flow rates of 5–7 mL/min, 500–600 mg BDS were collected per 15 min of burn. The DCM extracts of freshly prepared BDS exhibited an intense blue fluorescence under UV light. This is consistent with solubilization by DCM of PAHs formed during the combustion process and adsorbed to the surface of the BDS particles.

For undetermined reasons, occasional burns yielded particles that did not fluoresce in DCM, contained no detectable PAHs, and produced no cell fluorescence. These were not used.

Particle size distribution. Most particles in freshly generated BDS are of respirable size; > 90% of the collected particles are PM_{2.5} (Table 1).

Elemental analyses. Nearly 94% of BDS by weight is elemental carbon and approximately 2% is hydrogen, consistent with a polyaromatic composition of intact BDS. Together, nitrogen and sulfur account only for approximately 1% of the BDS components. Oxygen represents < 0.1% (Table 2). After extraction with DCM, the BDS takes on a more graphitic character compared with the

Table 3. ICP spectrometry analysis of elemental composition of BDS.

Element	Concentration (ppm)
Calcium	25
Iron	26
Potassium	4
Sodium	6
Phosphorus	19
Zinc	4

All analyses were in triplicate except for iron (*n* = 2).

nonextracted BDS, as indicated by the fact that the relative carbon content increases slightly and the relative hydrogen content drops below 1%.

The ICP analysis (Table 3) revealed that freshly generated BDS is not enriched in metals. For 52 of 64 elements, the levels were < 1 ppm. Of the remaining 12, calcium and iron (25 and 26 ppm, respectively) were the most prominent. Vanadium, chromium, and nickel, if present, were below the limits of detection with the analytical procedures used.

Percentage of adsorbed organic components. Extraction of BDS with DCM resulted in loss of $16.6 \pm 3.3\%$ (mean \pm SD; $n = 3$) of the initial weight of BDS. This loss is consistent with removal of aromatic compounds that had been adsorbed to the surface of the particles before extraction. However, small losses of ultrafine particles during filtration cannot be discounted.

GC/MS analysis of PAH components of BDS. Three batches of independently generated BDS $PM_{2.5}$ were analyzed by GC/MS after extraction with DCM. Thirteen of the most abundant PAH components, ranging from acenaphthylene (152 amu) to benzo[perylene]/indeno[perylene] (276 amu), are listed in Table 4. Four of these (anthracene, chrysene, benzopyrenes, and perylene; Table 4) were identified directly by comparison with results from their respective deuterated analogs. The values presented in Table 4 for all 13 PAHs are relative amounts, with each expressed as an intensity relative to anthracene- d_{10} . The PAHs were identified on the basis of their relative retention times (retention index) and by comparison with previously published results (Catalo 1998). The relative abundances of all 13 of these PAHs were consistent between batches. Similarly, there was very little difference in PAH composition between these three batches of BDS and the $PM_{2.5}$ sample from Table 1 (data not shown). There was insufficient material for GC/MS analysis in the two other fractions in Table 1. Many other PAHs also were detected but at lower levels than those of the 13 major components listed here. These results demonstrate that there is a characteristic chemical composition of BDS, regardless of size, that can be obtained reproducibly if consistent generation and collection schemes for BDS are followed.

Electron microscopy of BDS and of BDS-treated BEAS-2B cells. Under SEM, macroscopic BDS is composed of spherical, uniformly sized solid particles approximately 50–70 nm in diameter, which aggregate to form open, lacy clusters (Figure 1A). These results were confirmed with TEM analysis of soot collected directly on copper grids (Figure 1B), as well as by analysis of epoxy-embedded BDS samples (data not shown). Under TEM, the diameter of particles was 30–50 nm. The slightly larger

apparent diameter of the spherical particles (SEM vs. TEM) results from the 10–20-nm gold/palladium coating that had been applied to the particles during preparation for SEM.

Neither light microscope nor TEM analysis of BDS-treated cells yielded any evidence that the ultrafine particles were taken up by the cells during the same time period in which other cells from the same population displayed punctate fluorescence. There is, however, clear evidence from TEM that BDS ultrafine particles reach the cell surface. In Figure 1C, individual BDS particles that settled at the bottom of the culture dish are shown in immediate proximity to a BEAS-2B cell.

In vitro bioassay of BDS activity. Three milligrams of BDS, without carrier or solubilizing agent, sprinkled on the surface of BEGM overlying semiconfluent BEAS-2B cells, elicited a time-dependent set of fluorescence responses. Within 60–120 min, a uniform, diffuse blue fluorescence not localized in any organelles was detected in most cells. By 4 hr, the diffuse fluorescence was replaced by punctate fluorescence, that is, fluorescence localized in discrete, circular (1–2 μ m) cytoplasmic vesicles (Figure 2). No nuclear

fluorescence was detected. Fluorescence intensity in the cytoplasmic vesicles increased during the first 24 hr, then plateaued and remained constant for as long as 72 hr. Cells exposed to graphite did not fluoresce, nor did cells exposed to BDS from which adsorbed PAHs has been extracted with DCM. Extracts (DCM) of BDS—filtered through 0.45- μ m filters, dried, resuspended in DMSO, and diluted in BEGM—produced rapid fluorescence responses, including the appearance of punctate fluorescent in cytoplasmic vesicles within 30 min (data not shown). The time course of fluorescence responses of the cells combined with the evidence that the BDS particles are not taken up by the cells is consistent with PAHs being transferred to the plasma membrane from the surfaces of the ultrafine particles.

Intact BDS particles cannot be easily suspended in aqueous medium. Sonication was required to disperse the soot floating on the surface of the clear BEGM into the liquid to form an opaque black suspension. Less vigorous dispersion techniques were ineffective. Fluorescent cytoplasmic vesicles appeared more rapidly in cells exposed to sonicated BDS

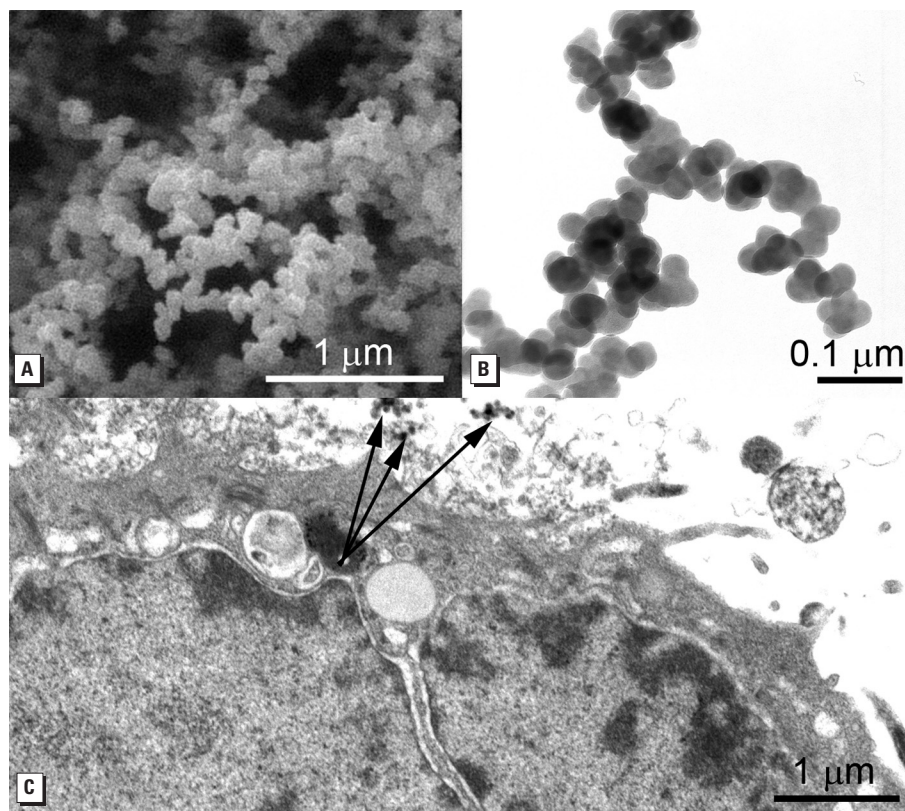


Figure 1. (A) An SEM image illustrating the lacy openwork character typical of the BDS aggregates; individual, solid, spherical particles, 50–70 nm in diameter, are the fundamental structural units of the aggregates. (B) A TEM image of BDS showing individual spheres, 30–50 nm in diameter, arranged in branching clusters. The difference in diameter of the spheres in the SEM versus TEM images results from the 10–20 nm gold/palladium conductive coating that was applied to the SEM samples. (C) A TEM image of a portion of the surface of a BEAS-2B cell with individual spherical particles, 30–50 nm in diameter, and small aggregates (arrows) immediately adjacent to the cell membrane. Cells were photographed after 42 hr exposure.

diluted with BEGM than in cells exposed to nonsonicated BDS (Table 5). The time required for 50% of the cells to display punctate fluorescence was 60, 90, and 150 min, respectively, for the 1:10 and 1:20 dilutions of sonicated samples and for the nonsonicated BDS samples. For the 1:50 and 1:100 dilution samples, the percentage of cells with punctate fluorescence never reached 50%, even after 24 hr. These results are consistent with increased numbers of ultrafine particles containing adsorbed PAHs being made available to the cells as a result of sonication.

Additional evidence that the fluorescence responses result from direct interaction of PAH-containing ultrafine particles with cells was obtained by plating BEAS-2B cells in 24-well dishes. Transwell inserts (0.4- μm pore) containing 0.3 mg nonsonicated BDS sprinkled onto 1 mL BEGM were placed in each well. Wells were examined at 4, 8, 24, and 48 hr. Fluorescent vesicles were visible at 4 hr in cells to which BDS had been added directly (no inserts) and at 18–48 hr in cells from the BDS/Transwell group. These results indicate that the fluorescence responses of cells in this case are dependent on accessibility of cells to particles of BDS that are < 0.4 μm in size. Crystals of BaP, which are more dense than the lacy, open aggregates of BDS, elicited punctate blue-violet fluorescence from cells within 4 hr, but only in cells immediately adjacent to BaP crystals that had dropped to the bottom of the dish. When the non-spherical BaP crystals, all larger than 0.4 μm ,

were floated on BEGM in Transwells, the cells did not fluoresce even after 48 hr (data not shown). In contrast, when crystalline BaP was dissolved first in DMSO and then mixed with BEGM (final BaP concentration = 40 μM) before addition to cells, all cells displayed punctate blue fluorescence within 2 hr.

Confirmation that the material adsorbed to the surface of the BDS ultrafine particles is inherently responsible for the cell fluorescence was obtained by solubilizing dried DCM extracts of BDS in DMSO, diluting them with BEGM, and adding them to Transwells. These extracts elicited diffuse fluorescence within 30–45 min and punctate fluorescence within 2 hr. When the same extracts were mixed with BEGM and added directly to wells lacking Transwells, punctate fluorescence was visible in cells by 30 min and in most cells by 3 hr. These results confirm that the fluorescence is due to uptake by the cells of PAHs desorbed from the surfaces of the ultrafine particles.

At 48 hr, the ODS disks and the cells from both the BDS/Transwell exposure and BDS/no Transwell exposure wells were rinsed, extracted with DCM, and analyzed with GC/MS. The major PAH peaks at 202 m/z , previously identified in extracts of BDS (Table 4), also are present in the extracts from the wells with BEAS-2B cells and the wells with the ODS disks (Figure 3). These peaks, however, are absent from wells to which BDS alone (without cells or the ODS disks) was added. These results, combined with *a*) the

absence of evidence for direct uptake of BDS ultrafine particles by the cells, *b*) the time lines for the development of fluorescence, and *c*) the very low levels of metals or other polar constituents in BDS, strongly suggest that nonpolar organic constituents adsorbed to the surface of combustion-derived ultrafine particles are transferred to the plasma membrane and subsequently to the cell interior.

Discussion

An extensive literature details a range of toxic responses, both *in vivo* and *in vitro*, after exposures to PAHs. In this article, we characterize physical and chemical properties of BDS, a complex airborne mixture of particles featuring adsorbed PAHs, produced as a result of incomplete combustion of BD, a major industrial petrochemical. Consideration of these properties is vital to understanding the processes whereby BDS and other ultrafine particulate combustion mixtures deliver and transfer potentially toxic components to target cells. We also describe a simple bioassay to test the effects of BDS and other combustion-derived, PAH-rich particle mixtures on putative target cells. Our results demonstrate that the overwhelming majority of freshly generated BDS particles are of respirable size, have a predictable chemical composition, and act to transport adsorbed, bioactive chemicals (primarily PAHs) to target cells. These results indicate that uptake of airborne ultrafine particles by target cells is not necessary for the particles to exert their toxic effects on the cells. These findings are especially timely in light of the current focus on toxicologic responses to inhaled airborne particulates.

The approach we used to generate BDS is similar to that described previously for soot generation during combustion of various hydrocarbons, including BD (Cole et al. 1984a, 1984b). Those authors focused on some of the less complex hydrocarbon combustion products (benzene, phenylacetylene) and also demonstrated that the key step in the process was most likely a free radical addition reaction of 1,3-butadienyl radical and acetylene. This type of reaction, which occurs in the high-temperature environment of a flame, is favored over a Diels-Alder reaction, which predominates at much lower temperatures. Our results and those of Catalo (1998) provide a

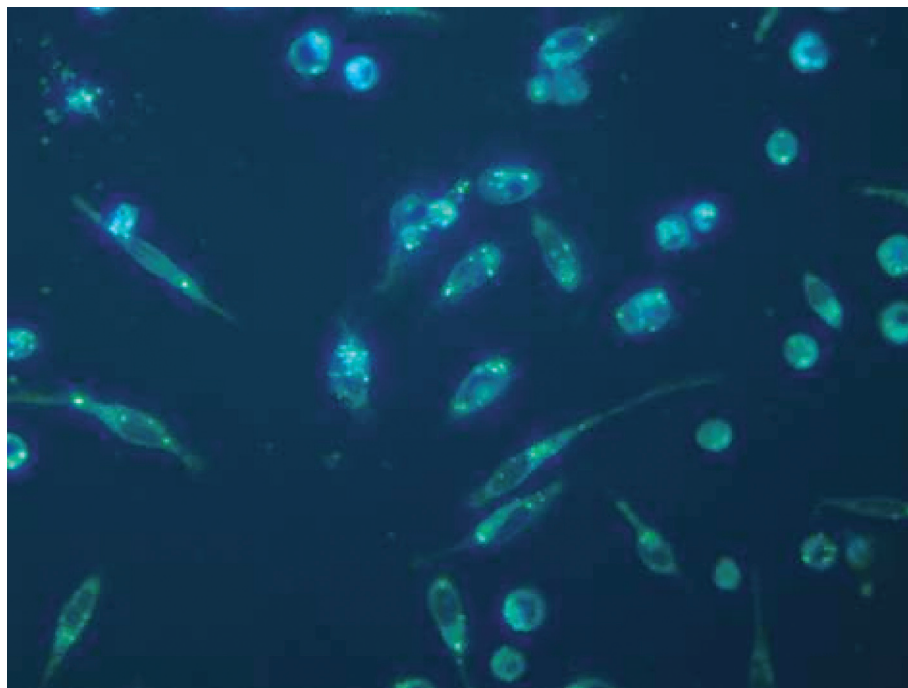


Figure 2. Fluorescence localized in punctate cytoplasmic vesicles of BEAS-2B cells. Cells were photographed 4 hr after BDS, without carrier, was sprinkled onto the surface of the BEGM overlying the cells. Excitation/emission wavelengths = 360/420 nm. Magnification, 400 \times .

Table 5. Time lag between the addition of diluted, sonicated BDS suspended in BEGM, and development of punctate fluorescence in BEAS-2B cells.

Dilution of sonicated BDS	Time to PF ₅₀
1:10	60 min
1:20	90 min
1:50	> 48 hr
1:100	> 48 hr

PF₅₀, punctate fluorescence in 50% of exposed BEAS-2B cells. The corresponding time lag for nonsonicated BDS sprinkled onto the surface of BEGM was 150 min.

more detailed and extensive description of the wide range of unsubstituted PAHs (Table 4) that are generated during combustion of C_4 hydrocarbons than was previously presented.

The elemental analyses emphasize the strong polyaromatic nature of BDS and the relative absence of ring substitution (Table 2). The very low levels of nitrogen, sulfur, and oxygen (Table 2) indicate that amines, nitro compounds, oxides of sulfur, quinones, hydroquinones, or semiquinones are not likely to be the BDS constituents that are primarily responsible for its biologic activity. None of these constituents was noted in multiple GC/MS analyses of BDS (data not shown). We have not yet investigated metabolism of BDS components by respiratory epithelial cells and so cannot address the question of whether oxidative products of that

metabolism are involved in the cells' responses to BDS exposure.

Figure 1A and 1B show that the dimensions of the solid spheres comprising the BDS particles are 30–50 nm in diameter. These dimensions agree with those for elementary soot particles from a variety of sources, including DEPs (Berube et al. 1999; Ishiguro et al. 1997; Murphy et al. 1999); aircraft fuel (Popovitcheva et al. 2000), cigarette smoke (Kendall et al. 2002), and carbon black (Freitas 2003; Lahaye and Ehrburger-Dolle 1994). The small size of the solid spheres corresponds to very high surface area per gram, maximizing the amount of PAH adsorbed per gram of soot. The small size also means that these particles have greater potential bioavailability.

As a source of potentially toxic particles of respirable size, BDS (and likely other

petrochemical soots, as well) rivals or exceeds a number of well-characterized mixtures of airborne particles, including tobacco smoke, diesel exhaust, urban reference dusts, and residual oil fly ash (ROFA). The comparisons to DEPs and ROFA are particularly informative in light of reported toxicologic responses to those particle mixtures. In some urban areas, DEPs, widely regarded as major agents of oxidative damage to cells of the respiratory system (Boland et al. 1999; Bonvallot et al. 2001; Kawasaki et al. 2001; Li et al. 2002), comprise 10–30% of the $PM_{2.5}$ and up to 50% of total ambient PM (U.S. EPA 2002). In a recent report that focused on mitochondrial dysfunction elicited by DEPs and ultrafine particles, Xia et al. (2004) concluded that the effects were “mediated by adsorbed chemicals” including polar (quinones) and (aromatic hydrocarbon) constituents, “rather than by the particles themselves.” For the PAHs that we have quantified in BDS (Table 4), the concentrations (milligrams per gram of BDS) are greater than or equal to values reported for the same components in DEP extracts (Tong et al. 1984). The respirable toxic particles in ROFA, a fuel oil combustion by-product from non-mobile sources, are relatively poor in organic components but rich in metals (Costa and Dreher 1997). Injury to airway cells and alterations in cytokine gene expression in response to ROFA exposure have been reported (Dreher et al. 1997; Dye et al. 1999; Samet et al. 2002). The elemental composition of BDS contrasts strikingly with that of ROFA. The iron level in BDS (Table 3) is three orders of magnitude lower than for ROFA (Costa and Dreher 1997). Further, vanadium and nickel levels in BDS are below the limits of detection (Table 3), whereas many of the effects of ROFA on respiratory cells have been attributed to its high vanadium content (Dye et al. 1999).

Appearance of fluorescent intracytoplasmic bodies (Figure 2) is a well-known response of cells and tissues to exposure to individual PAHs. Tissue fluorescence after injection of colloidal suspensions of BaP (Peacock 1940) and intracellular fluorescence localization of hydrocarbons, including BaP (Richter and Saini 1960), have long been recognized. In a later study, BaP solubilized in serum was taken up by HeLa and monkey kidney cells in culture (Allison and Mallucci 1964). At 24 hr, the cells exhibited a cytoplasmic granule fluorescence that the authors attributed to sequestration of BaP in lysosomes. Subsequently, internalization of high concentrations of BaP and its appearance as crystals in lysosomes of human foreskin fibroblasts 6–18 hr postexposure was described (Kocan et al. 1983). Other investigators, although confirming BaP uptake by cells, concluded that low to moderate levels of BaP were localized within lipid vesicles, not lysosomes

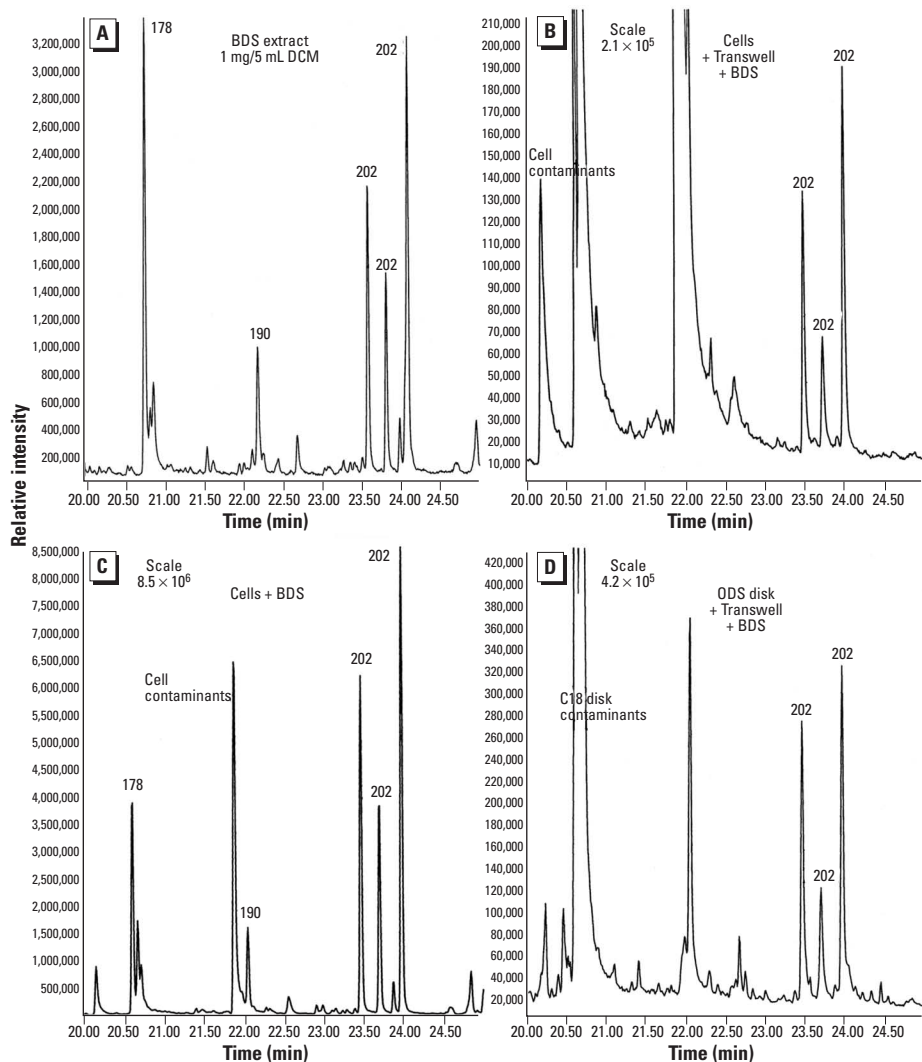


Figure 3. GC/MS ion chromatograms of (A) BDS extract (total ion), (B) cells exposed to BDS sprinkled on medium surface (selected ion monitoring (SIM)), (C) BDS added to a Transwell placed over cells (SIM), and (D) BDS added to a Transwell placed over an ODS disk (SIM). The same 202 m/z cluster was observed in all cases. Interference with monitoring of other PAH masses was due to cell or method contaminants, as noted. The GC/MS analyses were conducted as described in “Materials and Methods,” except that monitoring was in the selective ion mode.

(Plant et al. 1985). Intracellular lipid vesicles are likely repositories for hydrophobic PAHs. Preliminary results from our laboratory indicate that the punctate blue fluorescence is localized within vesicles that are stained with lipid dyes (Murphy G, Henk W, Barker S, Penn A, unpublished data).

The temporal development of the cells' fluorescence responses to ultrafine BDS particles and to crystalline BaP that has sunk to the bottom of the culture dish is consistent with direct transfer of adsorbed PAHs from the particle surface to the cells rather than by diffusion of dissolved PAHs to the cells. The solubility limit of PAHs in aqueous media is exceedingly small; a representative value is 2.3–3.0 ng/mL for BaP (Lakowicz et al. 1980; Muller 2002). This solubility limit is met in all of our preparations. The amount of soot used in our study ranged from 0.006 to 0.6 mg/mL BEGM. This corresponds to a range of 1×10^3 to 1×10^5 ng PAH/mL BEGM, an amount that exceeds the solubility of PAHs by several orders of magnitude. Thus, it can be assumed that the BEGM would be saturated with PAHs in all cases and that the fluorescence responses would not vary with the amount of soot added to the system. However, in our studies, the observed responses clearly correlate with the amount of soot added; the time required for punctate fluorescence to develop in the cells was shortened as the amount of soot particles per milliliter of suspension was increased (Table 5). Similarly, this time for development of punctate fluorescence was shortened in the case of BaP crystals that had been solubilized in DMSO before being mixed with the BEGM that was applied to the cells.

In the routine situation where BDS was sprinkled onto the surface of the medium, and not sonicated to form a suspension, most of the cells display punctate fluorescence after approximately 4 hr. This is consistent with transport of PAHs by the ultrafine particles directly to the surface of the cells (Figure 1C). As noted above, a soot sample collected by impaction is composed of solid, spherical particles (30–50 nm) arranged into lacy, open-work aggregates (Figure 1A,B; Berube et al. 1999). Although the density of these individual solid spheres is high, and the entire weight of the aggregates above the liquid line is supported by the spherical particles in direct contact with the liquid surface, the high surface tension of the liquid (and the hydrophobic particle surface) prevents individual spheres from piercing the liquid surface immediately (Cherry 1981). With time, the wettability of the spherical particles directly contacting the liquid surface is increased by the normal adsorption of moisture from the adjacent liquid surface, and the balance is changed so that individual spherical particles on the bottom of the aggregates can pierce the liquid

surface, detach, and sink because of their greater density.

The absence of light or electron microscopy evidence for direct cellular uptake of the BDS ultrafine particles or for involvement of endosomes in the process (Murphy G, Henk W, Barker S, Penn A, unpublished data) raises the question of how the BDS-associated PAHs traverse the plasma membrane and gain entry to the cells (Figure 3). Data from lipoprotein studies suggest that the PAH uptake can be accomplished by direct transfer of the PAHs from the BDS ultrafine particles to the plasma membrane, without the ultrafine particles themselves entering the membrane. Uptake of BaP from hydrophobic carriers by human fibroblasts and mouse macrophages occurred in the absence of endocytosis (Plant et al. 1985). In all cases, cellular uptake of BaP could be accounted for by a partitioning mechanism. Subsequently, Plant et al. (1987) described a three-compartment system to explain rapid membrane uptake of BaP from lipoproteins and phospholipid vesicles and for the much slower release of BaP from the cell membrane to intracellular sites. These proposed events are consistent with our findings of a lag between the appearance of a relatively rapid, diffuse fluorescence of BEAS-2B cells and the appearance of subsequent punctate cytoplasmic fluorescence.

Further support for cellular uptake of hydrophobic molecules but not of their carriers comes from studies on internalization of cholesterol esters by steroid-producing cells. The pathway for this uptake is termed "selective" and is distinct from receptor-mediated endocytosis. In the selective pathway, cholesterol esters, but not the lipoproteins that transport them, are internalized (Glass et al. 1983). The cholesterol esters become localized to intracellular perinuclear lipid droplets (Reaven et al. 1995). The transfer of cholesterol esters from the lipoproteins to the plasma membrane is temperature independent. The transfer from there to the perinuclear lipid vesicles does not require an intact Golgi apparatus or even an intact cytoskeleton but seems to require at least one sulfhydryl-containing protein at or very near the plasma membrane. Depletion of ATP from the cell seems not to interfere with the process, although depletion of glucose from the medium decreases efficiency of transfer to the cell interior (Reaven et al. 1996).

In our experiments, the cells are grown in a serum-free medium lacking lipoproteins. We propose that the BDS ultrafine particles serve as carriers for the PAHs, in a process analogous to that by which the lipoproteins in the "selective" transport process serve as carriers for the cholesterol esters. The energetics of the BDS-associated PAH uptake as well as the intracellular fate and toxicity of these PAHs currently are under investigation in our laboratory.

CORRECTION

The range of PAH per milliliter of BEGM (9×10^3 to 9×10^5 ng PAH/mL BEGM) in the "Discussion" of the manuscript originally published online was incorrect; it has been corrected here (1×10^3 to 1×10^5 ng PAH/mL BEGM).

REFERENCES

- Allison AC, Mallucci L. 1964. Uptake of hydrocarbon carcinogens by lysosomes. *Nature* 203:1024–1027.
- Bermudez E, Mangum JB, Wong BA, Ashgarian B, Hext PM, Warheit DB, et al. 2004. Pulmonary responses of mice, rats and hamsters to subchronic inhalation of ultrafine titanium dioxide particles. *Toxicol Sci* 77:347–357.
- Berube KA, Jones TP, Williamson BJ, Winters C, Morgan AJ, Richards JR. 1999. Physicochemical characterization of diesel exhaust particles: factors for assessing biological activity. *Atmos Environ* 33:1599–1614.
- Boland S, Baeza-Squiban A, Fournier T, Houcine O, Gendron MC, Chévrier M, et al. 1999. Diesel exhaust particles are taken up by human airway epithelial cells in vitro and alter cytokine production. *Am J Physiol Lung Cell Mol Physiol* 276:L604–L613.
- Bonvallot V, Baeza-Squiban A, Baulig A, Bruland S, Boland S, Muzeau F, et al. 2001. Organic compounds from diesel exhaust particles elicit a proinflammatory response in human airway epithelial cells and induce cytochrome p450 1A1 expression. *Am J Respir Cell Mol Biol* 25:515–521.
- Catallo WJ. 1998. Polycyclic aromatic hydrocarbons in combustion residues from 1,3-butadiene. *Chemosphere* 37:143–157.
- Catallo WJ, Kennedy CH, Henk W, Barker SA, Grace SC, Penn A. 2001. Combustion products of 1,3-butadiene are cytotoxic and genotoxic to human bronchial epithelial cells. *Environ Health Perspect* 109:965–971.
- Chalupa DC, Morrow PE, Oberdorster G, Utell MJ, Frampton MW. 2004. Ultrafine particle deposition in subjects with asthma. *Environ Health Perspect* 112:879–882.
- Cherry BW. 1981. The solid-liquid interface. In: *Polymer Surfaces*. Cambridge, UK:Cambridge University Press, 18–33.
- Cole JA, Bittner JD, Longwell JP, Howard JB. 1984a. Role of C4 hydrocarbons in aromatic species formation in aliphatic flames. *Chem Combust Processes* 249:3–21.
- Cole JA, Bittner JD, Longwell JP, Howard JB. 1984b. Formation mechanisms of aromatic compounds in aliphatic flames. *Combust Flame* 56:51–70.
- Costa DL, Dreher KL. 1997. Bioavailable transition metals in particulate matter mediate cardiopulmonary injury in healthy and compromised animal models. *Environ Health Perspect* 105(suppl 5):1053–1060.
- Dick CA, Singh P, Daniels M, Evansky P, Becker S, Gilmour MI. 2003. Murine pulmonary inflammatory responses following instillation of size-fractionated ambient particulate matter. *J Toxicol Environ Health A* 66:2193–2207.
- Dockery DW, Pope CA III, Xu X, Spengler JD, Ware JH, Fay ME, et al. 1993. An association between air pollution and mortality in six U.S. cities. *N Engl J Med* 329:1753–1759.
- Dreher KL, Jaskot RH, Lehmann JR, Richards JH, McGee JK, Ghio AJ, et al. 1997. Soluble transition metals mediate residual oil fly ash induced acute lung injury. *J Toxicol Environ Health* 50:285–305.
- Dye JA, Adler KB, Richards JH, Dreher KL. 1999. Role of soluble metals in oil fly ash-induced airway epithelial injury and cytokine gene expression. *Am J Physiol Lung Cell Mol Physiol* 277:L498–L510.
- Freitas RJ. 2003. Section 15.3.3.5 Amorphous Carbon Particles. In: *Nanomedicine, Volume IIA: Biocompatibility*. Georgetown, TX:Landes Bioscience, 121–126. Available: <http://www.nanomedicine.com/NMIIA/15.3.3.5.htm> [accessed 8 June 2005].
- Glass C, Pittman RC, Weinstein DB, Steinberg D. 1983. Dissociation of tissue uptake of cholesterol ester from that of apoprotein A-I of rat plasma high density lipoprotein: selective delivery of cholesterol ester to liver, adrenal, and gonad. *Proc Natl Acad Sci USA* 80:5435–5439.
- Ishiguro I, Takitori Y, Akihara K. 1997. Microstructure of diesel soot particles probed by electron microscopy: first observation of inner core and outer shell. *Combust Flame* 108:231–234.
- Kawasaki S, Takizawa H, Takami K, Desaki M, Okazaki H, Kasama T, et al. 2001. Benzene-extracted components are

- important for the major activity of diesel exhaust particles: effect on interleukin-8 gene expression in human bronchial epithelial cells. *Am J Respir Cell Mol Biol* 24:419–426.
- Ke Y, Reddel RR, Gerwin BI, Miyashita M, McMenamin M, Lechner JF, et al. 1988. Human bronchial epithelial cells with integrated SV40 virus T antigen genes retain the ability to undergo squamous differentiation. *Differentiation* 38:60–66.
- Kendall M, Tetley TD, Wigzell E, Hutton B, Nieuwenhuijsen M, Luckham P. 2002. Lung lining liquid modifies PM (2.5) in favor of particle aggregation: a protective mechanism. *Am J Physiol Lung Cell Mol Physiol* 282:L109–L114.
- Kocan RM, Chi EY, Eriksen N, Benditt EP, Landolt ML. 1983. Sequestration and release of polycyclic aromatic hydrocarbons by vertebrate cells *in vitro*. *Environ Mutagen* 5:643–656.
- Laden F, Neas LM, Dockery DW, Schwartz J. 2000. Association of fine particulate matter from different sources with daily mortality in six U.S. cities. *Environ Health Perspect* 108:941–947.
- Lahaye J, Ehrburger-Dolle F. 1994. Mechanisms of carbon black formation. Correlation with the morphology of aggregates. *Carbon* 32:1319–1324.
- Lakowicz JR, Bevan DR, Riemer SC. 1980. Transport of a carcinogen, benzo[a]pyrene, from particulates to lipid bilayers: a model for the fate of particle-adsorbed polynuclear aromatic hydrocarbons which are retained in the lungs. *Biochim Biophys Acta* 629:243–258.
- Li N, Wang M, Oberley TD, Sempf JM, Nel AE. 2002. Comparison of the pro-oxidative and proinflammatory effects of organic diesel exhaust particle chemicals in bronchial epithelial cells and macrophages. *J Immunol* 169:4531–4541.
- Muller P. 2002. Potential for Occupational and Environmental Exposure to Ten Carcinogens in Toronto. Toronto, Ontario, Canada:ToxProbe Inc.
- Murphy SA, Berube KA, Richards RJ. 1999. Bioreactivity of carbon black and diesel exhaust particles to primary Clara and type II epithelial cell cultures. *Occup Environ Med* 56:813–819.
- Nemmar A, Hoylaerts MF, Hoet PH, Nemery B. 2004. Possible mechanisms of the cardiovascular effects of inhaled particles: systemic translocation and prothrombotic effects. *Toxicol Lett* 149:243–253.
- Nemmar A, Vanbilloen H, Hoylaerts MF, Hoet PH, Verbruggen A, Nemery B. 2001. Passage of intratracheally instilled ultrafine particles from the lung into the systemic circulation in hamster. *Am J Respir Crit Care Med* 164:1665–1668.
- OSHA. 2004. Safety and Health Topics: 1,3-Butadiene. Washington, DC:Occupational Safety and Health Administration. Available: <http://www.osha.gov/SLTC/butadiene/> [accessed 8 June 2005].
- Peacock PR. 1940. Biophysical factors influencing the absorption and distribution of benzopyrene and their bearing on the mechanism of carcinogenesis. *Am J Cancer* 40:251–254.
- Peters A, Wichmann HE, Tuch T, Heinrich J, Heyder J. 1997. Respiratory effects are associated with the number of ultrafine particles. *Am J Respir Crit Care Med* 155:1376–1383.
- Plant AL, Benson DM, Smith LC. 1985. Cellular uptake and intracellular localization of benzo(a)pyrene by digital fluorescence imaging microscopy. *J Cell Biol* 100:1295–1308.
- Plant AL, Knapp RD, Smith LC. 1987. Mechanism and rate of permeation of cells by polycyclic aromatic hydrocarbons. *J Biol Chem* 262:2514–2519.
- Pope CA III, Burnett RT, Thun MJ, Calle EE, Krewski D, Ito K, et al. 2002. Lung cancer, cardiopulmonary mortality, and long-term exposure to fine particulate air pollution. *JAMA* 287:1132–1141.
- Popovitchcheva OB, Persiantseva NM, Trukhin ME, Rulev GB, Shonija NK, Buriko YY, et al. 2000. Experimental characterization of aircraft combustor soot: microstructure, surface area, porosity, and water absorption. *Phys Chem Chem Phys* 2:4421–4426.
- Reaven E, Tsai L, Azhar S. 1995. Cholesterol uptake by the ‘selective’ pathway of ovarian granulosa cells: early intracellular events. *J Lipid Res* 36:1602–1617.
- Reaven E, Tsai L, Azhar S. 1996. Intracellular events in the “selective” transport of lipoprotein-derived cholesteryl esters. *J Biol Chem* 271:16208–16217.
- Richter KM, Saini VK. 1960. U-V-fluorescence studies on the *in vitro* intracellular accumulation of carcinogenic hydrocarbon. *Am J Anat* 107:209–235.
- Samet JM, Dominici F, Currier FC, Coursac I, Zeger SL. 2000. Fine particulate air pollution and mortality in 20 U.S. cities, 1987–1994. *N Engl J Med* 343:1742–1749.
- Samet JM, Silbajoris R, Huang T, Jaspers I. 2002. Transcription factor activation following exposure of an intact lung preparation to metallic particulate matter. *Environ Health Perspect* 110:985–990.
- Schwartz J, Dockery DW, Neas LM. 1996. Is daily mortality associated specifically with fine particles? *J Air Waste Manag Assoc* 46:927–939.
- Tong HY, Sweetman JA, Karasek FW, Jellum E, Thorsrud A. 1984. Quantitative analysis of polycyclic aromatic hydrocarbons in diesel exhaust particulate extracts by combined chromatographic techniques. *J Chromatog* 312:183–202.
- U.S. EPA. 1991. National Ambient Air Quality Standards for Airborne PM. Washington, DC:U.S. Environmental Protection Agency.
- U.S. EPA. 1997. National Ambient Air Quality Standards for Airborne PM. Washington, DC:U.S. Environmental Protection Agency.
- U.S. EPA. 2002. Health Assessment for Diesel Exhaust. Washington, DC:U.S. Environmental Protection Agency.
- Xia T, Korge P, Weiss JN, Li N, Venkatesen MI, Sioutas C, Nel A. 2004. Quinones and aromatic chemical compounds in particulate matter induce mitochondrial dysfunction: implications for ultrafine particle toxicity. *Environ Health Perspect* 112:1347–1358.